Published in final edited form as:
Int J Neural Syst. 2009 June ; 19(3): 173–196.

Control of Synchronization of Brain Dynamics Leads to Control of Epileptic Seizures in Rodents

Levi B. Good[*],
Harrington Department of Bioengineering, Arizona State University, Tempe, Arizona, USA, Department of Neurology Research, Barrow Neurological Institute, St. Joseph's Hospital & Medical Center, Phoenix, Arizona, USA

Shivkumar Sabesan,
Department of Electrical Engineering, Arizona State University, Tempe, Arizona, USA

Steven T. Marsh,
Department of Neurology Research, Barrow Neurological Institute, St. Joseph's Hospital & Medical Center, Phoenix, Arizona, USA

Kostas Tsakalis,
Department of Electrical Engineering, Arizona State University, Tempe, Arizona, USA

David Treiman, and
Department of Neurology, St. Joseph's Hospital & Medical Center, Phoenix, Arizona, USA, Harrington Department of Bioengineering, Arizona State University, Tempe, Arizona, USA

Leon Iasemidis
Harrington Department of Bioengineering, Arizona State University, Tempe, Arizona, USA, Leon.Iasemidis@asu.edu, http://www.fulton.asu.edu

Abstract

We have designed and implemented an automated, just-in-time stimulation, seizure control method using a seizure prediction method from nonlinear dynamics coupled with deep brain stimulation in the centromedial thalamic nuclei in epileptic rats. A comparison to periodic stimulation, with identical stimulation parameters, was also performed. The two schemes were compared in terms of their efficacy in control of seizures, as well as their effect on synchronization of brain dynamics. The automated just-in-time (JIT) stimulation showed reduction of seizure frequency and duration in 5 of the 6 rats, with significant reduction of seizure frequency (>50%) in 33% of the rats. This constituted a significant improvement over the efficacy of the periodic control scheme in the same animals. Actually, periodic stimulation showed an increase of seizure frequency in 50% of the rats, reduction of seizure frequency in 3 rats and significant reduction in 1 rat. Importantly, successful seizure control was highly correlated with desynchronization of brain dynamics. This study provides initial evidence for the use of closed-loop feedback control systems in epileptic seizures combining methods from seizure prediction and deep brain stimulation.

Keywords

Seizure; prediction; deep brain stimulation; nonlinear; control

Correspondence to: Leon Iasemidis.
[*]Present address: Department of Neurology, University of Texas Southwestern Medical Center, 5323 Harry Hines Blvd, Mail Code 8813, Dallas, Texas, 75390, USA.

1. Introduction

Epilepsy is the second most common neurological disorder after stroke, and affects at least 50 million people world-wide. Approximately 60% of new onset epilepsy cases respond to existing antiepileptic drugs (AEDs), however 40% are pharmacoresistant (intractable), with seizures that cannot be fully controlled with available medical therapy or without unacceptable side effects.[1] Thus, there are nearly 20 million people world-wide for whom the development of more effective epilepsy treatment paradigms would be greatly beneficial.

Currently, antiepileptic drugs are the principal form of chronic epilepsy management. However, in addition to the lack of efficacy in nearly one-third of epileptic patients, there are substantial side effects and morbidity associated with the use of antiepileptic drugs, especially when polypharmacy is required. While surgical removal of the seizure focus is an important and effective therapeutic intervention for patients with difficult to control epilepsy, resective surgery is unlikely to replace chronic treatment as the primary mode of medical epilepsy management. There exists a large population of patients in whom surgical resection is not possible. This can be due to the presence of multiple epileptic foci, seizure foci located in non-resectable areas of the brain (such as eloquent cortex associated with language or speech processing), or the absence of a well-defined seizure focus like in primary generalized epilepsies.

Electrical stimulation paradigms, as a means of seizure control, have the advantage of not producing the systemic and central nervous system side effects which are seen frequently with antiepileptic drugs. The vagus nerve stimulator (VNS) as an antiepileptic device was approved by the US Food and Drug Administration in 1997. More than 30,000 VNS devices have been implanted in patients with epilepsy throughout the world. One-third of these patients experience at least a 50% reduction of seizure frequency, but fewer than 10% become seizure-free.[2] This device works primarily by periodic stimulation of the left vagus nerve in the neck, however, it is possible for the patient to activate the stimulator with a magnet if he or she has a seizure aura sufficiently early to allow activation before mental impairment by the upcoming seizure.

Deep brain stimulation (DBS), principally of thalamic structures, has also been reported to reduce seizure frequency in humans.[3–6] Chkhenkeli *et al.* reported the inhibitory effects of electrical stimulation at the head of the caudate nuclelus, cerebellar dentate nucleus, thalamic centromedian nucleus and neocortical and temporal lobe mesiobasal epileptic foci in 150 patients.[7] In this study, chronic brain stimulation was performed on 54 of these patients which resulted in seizure elimination in 48%, improvement of seizures in 43%, and no improvement in 9% of the patients. Suppression of sub-clinical epileptic discharges and a reduced frequency of generalized, complex partial, and secondary generalized seizures was noted with stimulation of 4– 8 Hz in the head of the caudate nucleus and with 50–100 Hz in the cerebellar dentate nucleus. Centromedian nucleus (CM) stimulation at 20–130 Hz desynchronized the EEG and suppressed partial motor seizures. The stimulus was either delivered as a continuous regimen (12–14 hours/day) or intermittent stimulation (10 min “on” then 15–20 min “off”, for 12–14 hours/day; 20–30 minutes on, 3 or 4 times a day; 5 min “on” then 5 min “off”, 3 or 4 times a day).[7]

Deep brain stimulation has also shown promising results in controlling epileptic seizures in several animal models of epilepsy with high frequency stimulation targeting the subthalamic nucleus, anterior thalamic nucleus, caudal superior colliculus, substantia nigra, and hippocampus.[8–18] In all these investigations, stimulation parameters were in the following

ranges: frequency from 50 to 230 Hz, bipolar constant current pulses of duration 30 to 1000 μsec, with current intensities from 0.1 to 2 mA. Low frequency (between 1 to 30 Hz) stimulation resulted in increase of seizure susceptibility.

Two clinical trials of DBS for epilepsy management are currently underway in the United States, one being conducted by Medtronic and the other by NeuroPace, each with its attendant risk and expense. Surgical implantation of stimulating electrodes into the thalamus or the seizure focus (Medtronic study) and into the seizure focus (Neuropace study) is required. Like the VNS device, the Medtronic DBS device[4,19] delivers periodic (e.g., 1 min of trains of high frequency 145–175 Hz biphasic square pulses stimuli, with 5 minutes OFF time) stimuli to the anterior thalamus, independent of the presence or absence of seizure activity. Efficacy results from this stimulation scheme vary wildly and, among other factors, they apparently depend heavily on the site of stimulation, and are masked by AEDs patients continue to take after implantation of DBS. Responsive neurostimulation is an alternative scheme to the above periodic stimulation scheme. Again, a predetermined (independent of the state of the brain) form of stimulus is administered to “focal” areas. The difference is that the administration of the stimulus (stimulation) is not periodic any more. It is delivered either at the onset of an impending seizure, therefore limiting its efficacy to only abate seizures after they have started and does not directly treat the underlying interictal/preictal pathology that eventually leads to seizures,[20] and/or at points in time where epileptiform waveforms are detected by software (Neuropace study[21]). This software should be highly patient-dependent, handles a plethora of at times unmanageable and pretty subjective parameters (as well as rules for their interaction) that need to be identified from pre-recorded training datasets from each patient, and does not guarantee a satisfactory performance in a typically non-stationary and difficult to anticipate EEG.[22,23] Besides some pitfalls in the reporting of results (e.g., instead of excluding patients from statistical evaluation when they did not exhibit any clinical seizures with stimulation ON or OFF in the testing phase, patients were included as 100% responders[20]), this scheme of stimulation appears to be more promising than the periodic one. Even though no study has yet demonstrated a clearly better efficacy in seizure control of a just-in-time (JIT) neurostimulation than a corresponding periodic scheme, JIT has considerable theoretical and practical advantages.

The theoretical advantages have been described in the past (e.g., better efficacy for seizure control),[22] and are now directly supported by results from our recent theoretical (computer simulation) investigations in ictogenesis.[24–28] Our preliminary experimental results also support these conjectures.[29–33] On the other hand, in addition to better efficacy, the practical advantages are related to the economy of power JIT stimulation may offer by having the stimulator ON less frequently and for a shorter duration (only intermittently, and only when needed). This may result into longer battery life, reduced size of implanted device and reduction of side effects from excessive exposure of the brain to stimulation (issues that are closely related to patient safety too). In the ideal JIT, the stimulus would be activated sufficiently early (actually, as long before a seizure onset as possible) to prevent the brain's route towards a seizure. This requires the ability to detect EEG changes predictive of an impending seizure in the preictal period (minutes to hours before a seizure's occurrence), and to then deliver a control stimulus long prior to the actual occurrence of a seizure with a very well-defined goal, for example to desynchronize the brain dynamics (as we herein show).

In the last decade, substantial progress has been made towards seizure prediction by the introduction of novel concepts and measures from spatiotemporal state transitions in nonlinear systems into the study of the human brain. It has now become evident that epilepsy is a dynamical disorder of the brain. The hallmark of this line of research is the ability to predict epileptic seizures (in the order of tens of minutes) prior to their clinical or

electrographic onset. In 1988, Iasemidis *et al.* reported the first investigation into clinical epilepsy within the framework of nonlinear dynamics.[34] Reports on the nonlinear nature of the EEG in epilepsy followed.[35–47] Through the use of Lyapunov exponents, we showed that seizures are consistent with transitions of the epileptic brain from its less ordered (chaotic) state to a more ordered state (less chaotic) and back to a less ordered (chaotic) postictal state along the lines of chaos-to-order-to-chaos transitions. Subsequently, the existence of long-term preictal periods (order of minutes) was shown using nonlinear dynamical analysis of EEG from subdural arrays and raised the possibility of designing seizure prediction algorithms via monitoring the temporal evolution of the short-term maximum Lyapunov exponents (STL_{max}). More recently, in patients with focal temporal lobe epilepsy (TLE), it was shown that the observed preictal dynamical entrainment of normal brain sites with the focus is typically reset in the immediate postictal period.[48] This may well indicate that a successful seizure therapy should concentrate on long-before-seizure-occurrence resetting of the dynamical recruitment of the "normal" brain sites by the focus. Even though in the past we have used the term "dynamical entrainment" to characterize the transition towards an epileptic seizure, in the rest of this paper we are using the term "dynamical synchronization" to denote the synchronization that results from such an entrainment of the "normal" brain sites by the epileptogenic focus.

The current study was designed to test the following two hypotheses: (1) that an epileptic seizure will be prevented if an electrical stimulation successfully resets the observed pathological preictal synchronization of the brain, and (2) periodic stimulation performs worse than an automated justin-time (JIT) stimulation of the brain at warnings of an impending seizure. In Section 2, the employed methodology to generate seizures in rats, the seizure prediction methods utilized, as well as the design and implementation of the automated JIT stimulation system are discussed. Deep brain stimulation with parameters comparable to ones in the literature was used and incorporated in a stand-alone system. An evaluation of this system in terms of its efficacy in seizure prediction and control of brain dynamics is shown in Section 3, followed in Sections 4 and 5 by a discussion and conclusions of its possible use as an alternative treatment modality for the pharmacologically refractory epilepsy patient.

2. Methods

2.1. Animal model of chronic epilepsy

Animal models of chronic epilepsy that is induced by an episode of acute status epilepticus (SE) fulfill many characteristics for identification of effective therapeutic interventions. In this study, the lithium-pilocarpine (LP) model of acute SE in rats was chosen as the model for development of chronic epilepsy due to its similarities with temporal lobe epilepsy (TLE) in patients.[49–50] TLE is one of the most common forms of intractable epilepsy. Thus the LP model is an appropriate choice to study new treatments for the pharmaco-resistant patient (intractable epilepsy).

Injection of lithium chloride, followed 24-hours later by pilocarpine (a muscarinic agonist), in rats induces generalized convulsive status epilepticus that can last for several hours. Many researchers report the LP rat model to have a latent period (from the episode of SE to the development of recurrent spontaneous seizures — chronic epilepsy) typically lasting 4–6 weeks.[49–55] As in patients, the neuropathology includes hippocampal sclerosis, as well as neuronal damage to other limbic structures, such as the amygdala, thalamus, and entorhinal cortex; however, the extent of damage is usually more apparent and extensive than the one seen in patients.[55]

The spontaneous recurrent seizures seen in these chronic epileptic rats have features that both electrographically and behaviorally resemble complex partial seizures originating in the limbic structures with secondary generalization (also observed in TLE patients). Electrographically, these seizures show spike and wave discharges in the recorded EEG which spread from the limbic brain structures out to the cortex. As in TLE patients, these spike and wave discharges evolve as the seizure progresses and similarly show a marked slowing of EEG activity at seizure offset. Behaviorally, secondary generalization of the seizure in these rats results in both tonic posturing and a clonic shaking behavior of the limbs and face, typically with subsequent loss of balance and awareness of their surroundings, again similar to behavior observed in TLE patients.

Male Sprague-Dawley rats (200–225 g), obtained from Harlan Labs (Madison, WI), were used for the study. The experiments and data collection were conducted in the Laboratory for Translational Epilepsy Research at Barrow Neurological Institute and approved by the Institutional Animal Care and Use Committee. The algorithms for the analysis of the data were developed in the Brain Dynamics Lab at Arizona State University. An episode of acute SE, utilizing the LP model, was used to generate a subsequent state of chronic epilepsy with spontaneous recurring seizures. In our LP model formulation, rats received an intraperitoneal (IP) injection of 3 mmol/kg lithium chloride (Sigma) mixed in sterile 0.9% saline at a dose volume of 1 ml/kg, 24 hours prior to a subcutaneous injection of 30 mg/kg pilocarpine (Sigma) mixed in sterile 0.9% saline at a dose volume of 1 ml/kg.

Rats entered SE approximately 20 minutes after pilocarpine injection. Evidence of SE was noted behaviorally by the presence of a Racine level 5 seizure (rearing with loss of balance).[56] Once SE was established (60 minutes of continuous seizure activity), each rat received an IP injection of 15 mg/kg of acepromazine, at a dose volume of 1.5 ml/kg, in order to aid in survival. Rats were allowed to spontaneously recover from SE, which may take up to 24 hours. For the initial 72 hours following the episode of SE, rats were fed a diet of rat biscuits supplemented with a Transgel pack (Charles River Labs, Wilmington, MA). Rats were housed individually with a 12 hour light-dark cycle and monitored daily by visual inspection for the presence of spontaneous seizures.

2.2. Surgical techniques/placement of electrodes

Three to four weeks after the insult of SE, rats (by then weighing 350–400 g) were implanted with a six-microwire monopolar electrode array targeted for EEG recording in: (a) four cortical locations (from Bregma: A-P 2.0-mm, lateral ± 3.0-mm and A-P −4.0, lateral ± 3.0-mm to depth 1.0-mm), and (b) two hippocampal locations (A-P −5.6-mm, lateral ± 4.5-mm, to depth of 5.0-mm). Two Teflon coated tungsten bipolar twisted stimulating electrodes were also inserted, targeting the centromedial thalamic nucleus (A-P −2.5-mm, lateral ± 1.5-mm, to depth 5.9-mm under a 10° lateral angle). During the surgical implantation of the electrodes, rats were anesthetized with an intramuscular injection of an anesthetic cocktail consisting of 50 mg/kg ketamine, 10 mg/kg xylazine, and 1 mg/kg acepromazine, and maintained with a 20% booster dose of the cocktail every 45-minutes during the surgery or as necessary.

Aseptic techniques were employed during the surgical process. The hair was shaved from the base of the skull to the nasium and the eyes coated with Lacrilube gel. Rats were then mounted in a stereotaxic frame (Kopf Instruments, Tujunga, CA) and the surgical area swabbed with 70% ethanol and Betadine. The skull was subsequently exposed by a single anterior-posterior scalpel incision and the periostium scraped free from the cranium. Electrode locations were identified stereotaxically from Bregma where a 1-mm craniotomy at each position was created with a stereotaxic drill.

Once all electrode positions were exposed, the monopolar six-electrode array was implanted and temporarily held secure by super glue. The bipolar twisted stimulation electrodes were then implanted into the centromedial nucleus of the thalamus under a lateral angle of 10 degrees. One reference and one ground electrode (#0–80 stainless steel screws), were implanted over the olfactory bulb and cerebellum respectively along with four additional anchor screws to hold the implant in place. Once all electrodes and anchors were in position, the connector was positioned in an anterior-posterior arrangement and the implant secured with dental acrylic. Each end of the incision was then sutured and the rat removed from the stereotaxic frame and allowed to recover in individual Plexiglass cages for at least 48 hours prior to further handling.

A histological evaluation of the stimulation electrode placement was attempted for each rat after the end of the experiments. Briefly, rats were anesthetized followed by cardiac perfusion with 4% paraformaldehyde and their brains were removed. Coronal sections (30 μm) were made using a microtome and stained with hematoxylin and eosin to verify electrode tip placement. In most of the rats, while there was an appearance of electrode tracts leading toward the central thalamus, the exact tip placement was not able to be determined due to a large amount of tissue tears and damage resulting from removal of the electrodes and connector piece, mostly by the rats towards the end of this lengthy study.

2.3. EEG recording

All electroencephalographic (EEG) data in the study were recorded on a Beehive Millenium® LTM EEG machine (Grass-Telefactor Inc., West Warwick, RI). Recorded EEG data were band-pass filtered at 0.3 to 70 Hz, including a 60 Hz notch filter, and stored to a network hard disc in 1-minute file segments. All recordings were done in a referential mode, with the electrode over the olfactory bulb as the reference.

At least 48 hours following electrode implantation, rats were connected to the EEG machine through an interposed commutator system that allowed free movement of the animal in each cage to access food and water. All EEG data were continuously recorded over days with concurrent real-time nonlinear dynamical analysis of the recorded EEG on an adjacent personal computer.

2.4. Nonlinear dynamics of EEG

2.4.1. Short-term Lyapunov exponents—The EEG is the output of a complex multidimensional system (brain) and has statistical properties that depend both on time and space.[57] Bursting behavior, intermittent spike phenomena, and amplitude-dependent frequency behavior are among typical patterns that have proven difficult to understand with current statistical techniques. Neurons in the brain are densely interconnected and the EEG recorded from one site is inherently related to activity recorded at another, although the neural activity recorded from these two sites may functionally interact at different points in time. Because of this behavior, the EEG is considered a multivariable non-stationary time series. While the nervous system involves an enormous number of interrelated variables, almost impossible to all be measured, it is theoretically possible to make quantitatively meaningful inferences about the underlying global dynamics through monitoring of a subset of a few critical variables for long periods of time.[58]

A well-established technique for visualizing, and then quantifying, the dynamical behavior of a multivariate system is to generate its portrait in the space of its states. Each instantaneous state of the system in the state space is represented as a vector with components the time dependent variables of the system. These time-dependent vectors are

plotted sequentially in the state space and capture the evolution of the state of the system over time.[59] This process is called embedding.

Since the ictal state (during the period of a seizure) is more ordered (less chaotic), with reduced complexity (correlation dimension between 2 and 3) than the interictal state (during periods between seizures),[60] embedding of the recorded EEG from one brain site in a 7-dimensional state space using the method of delays may capture the dynamics of the ictal state.[61] In such an embedding, each state at time t is represented by a vector $X(t)$, whose components are the delayed versions of an original single-channel EEG time series $x(t)$, and is described by:

$$X(t)=[x(t), x(t+\tau), x(t+2\tau), \ldots, x(t+(p-1)\tau)] \quad (1)$$

where $p = 7$ is the embedding dimension of the state space and τ is the embedding time delay calculated from the first local minimum of the mutual information (MI) of the segment of the EEG signal we embed. Although the embedding dimension of the interictal state is expected to be higher than that of the ictal state, a constant embedding dimension $p = 7$ has been used to reconstruct all relevant state spaces over the ictal and interictal periods at different brain locations. The advantages of using such a small embedding dimension are that: (a) irrelevant information to the epileptic transition in dimensions higher than 7 would have much not influence on the values of the estimated dynamical measures, and (b) estimation of the dynamical measures suffers less from the small number of data points available per moving window (short windows are used to address the nonstationarity of the EEG). The disadvantage is that critical information about the transition to seizures, that may exist in dimensions higher than 7, would not be captured.

Measures of chaos, that measure the rate of generation of new information in stationary data (e.g. data from chaotic attractors), had been defined in the past.[62] Based on these measures, Iasemidis *et al.* developed indices that can be applied to nonstationary data and approximately measure the existence of chaos in these data. The indices were called short-term maximum Lyapunov exponents (STL_{max}).[60,61] Sensitivity analysis of the STL_{max} measure, in terms of the minimum required length of EEG segments from epileptic patients to produce robust and distinct STL_{max} values between interictal and ictal states, has shown that EEG segment's duration of 10.24 sec is a reasonable choice.[61]

2.4.2. Spatial synchronization of dynamics—As measures of dynamics, the STL_{max} values have been estimated over time, one value per each of sequential non-overlapping EEG epochs of 10.24 sec in duration from each of multiple electrode sites, thus creating a set of STL_{max} profiles (one STL_{max} profile per recording site) over time. These profiles characterize the spatio-temporal chaotic signature of the epileptic brain. Based on the Student's paired t-test of m degrees of freedom (independence and Gaussian conditions are satisfied — see[63]), a statistical distance T_{ij}^{t} between the STL_{max} profiles of pairs of electrode sites i and j is used to quantify the level of synchronization of dynamics between these sites within a time window of $w(t, t + m \cdot 10.24 \text{ sec})$, where $m = 60$ STL_{max} values (that is, window length of approximately 10 minutes).

The desynchronization condition between electrode sites i and j, as determined by the paired t-test, is:

$$T_{ij}^{t} > t_{\alpha/2,m-1} = T_{th} \quad (2)$$

where $t_{\alpha/2,m-1}$ is the $100 \cdot (1 - \alpha/2)\%$ critical value of the t-distribution with $m - 1$ degrees of freedom. If $T_{ij}^{t} \leq t_{\alpha/2,m-1}$ (which means that we do not have satisfactory statistical evidence at the α level that the differences of $STL_{\max}$ values between electrode sites i and j within the time window $w(t)$ are not zero), we consider that sites i and j are dynamically synchronized (entrained) with each other at time t. Using $\alpha = 0.01$ and $m = 60$, the synchronization threshold $T_{th} = 2.662$. On the other hand, if $T_{ij}^{t} > t_{\alpha/2,m-1}$ (which means that we have satisfactory statistical evidence at the α level that the differences of $STL_{\max}$ values between electrode sites i and j within the time window $w(t)$ are not zero), we consider that sites i and j are dynamically desynchronized (disentrained) with each other at time t.

Finally, in the rest of the paper, we call T-index(t) the spatial average of T_{ij}^{t}s, that is, the average of T_{ij}^{t} values from a set of (i, j) pairs of sites at time t. Thus, T-index profiles of a set (tuple) of electrode sites are estimated as the average of all possible pairs (i, j) between electrode sites in the tuple, and as such they constitute average spatial synchronization of brain dynamics profiles over space and time. Evidently, low values of T-index denote synchronization, while high values desynchronization of dynamics.

2.4.3. Resetting of dynamics at seizures—Desynchronization of synchronized brain dynamics around epileptic seizures has been observed and analyzed in patients with epilepsy in the past. We have called this phenomenon seizure resetting, and we have shown that it predominantly occurs at seizures than at any other point in the interictal period.[48] We have observed the same phenomenon in epileptic rats. Figure 1 shows the details of resetting around a typical seizure in one of the rats in this study after it became chronically epileptic. We notice that a) triplets of electrode sites exist that are dynamically synchronized (their corresponding T-indices are continuously less than $T_{th} = 2.662$) long before (about 40 minutes) the depicted seizure (e.g. the tuple of left frontal F3, right hippocampal RH, left hippocampal LH electrodes, and the tuple of left frontal F3, right hippocampal RH, right parietal P4), and b) the synchronized tuples desynchronize (their corresponding T-indices become greater than $T_{th} = 2.662$) within minutes after the end of the seizure. It is to be understood that seizures may not always be able to reset the brain. For example, seizures in status epilepticus typically cannot reset the brain.[23]

2.4.4. Resetting of dynamics at stimulation—Motivated by the above findings in humans and rats, that is the existence of long-term preictal dynamical synchronization and fast postictal desynchronization, we have hypothesized in the past that intervention with a potential to reset the synchronization of the epileptic brain dynamics early in the preictal period could avert the occurrence of the impending seizure.[22] In Fig. 2, an example of resetting of brain sites by electrical stimulus is shown in terms of the corresponding T-index of triplets of electrode sites. The T-index is estimated every 10.24 sec, from overlapping 10 min windows running in the $STL_{\max}$ profiles of the pairs of brain sites (i, j) included in the estimation of T-index. In this case, evidence of desynchronization (increase in T-index above the synchronization threshold), following the stimulus artifact zone is present for nearly 30 minutes after the end of stimulus. Desynchronization of brain dynamics was most apparent at the highest tolerated amplitude (non-seizure inducing), with either 130 or 200 Hz. It is to be understood that stimuli of this form are not always successful in resetting the brain.

2.5. Seizure prediction in rats

The seizure prediction scheme described by Iasemidis *et al.*[63,64] was used in this study. This scheme follows the amount of dynamical synchronization (*T*-index) of brain sites over time.

Issue of a seizure warning—The progressive convergence of the STL_{max} Lyapunov exponents over time is the basis for a seizure warning to be issued. This is achieved by setting two thresholds in the *T*-index profiles: a large upper threshold (UT), which corresponds to desynchronization with $p < 0.01$, as well as the low (LT) synchronization threshold (LT = T_{th}). In this prediction scheme, a seizure warning is only issued when the *T*-index of selected critical sites makes a transition from above UT to below LT (see Fig. 1). Since not all brain sites may progressively be synchronized prior to a seizure, the selection of the ones that are synchronized (critical sites) is a global optimization problem with a goal to minimize the distance between the STL_{max} dynamical measures at these sites.

Selection of critical sites—The solution to this problem, and its application prospectively to seizure prediction schemes, has been previously described.[65,66] Briefly, let's consider the integer bivalent 0–1 problem:

$$\min x^t T x, \text{ with } x \in \{0, 1\}^n,$$
$$\text{Subject to the constraint } \sum_{i=1}^{n} x_i = k,$$

where *n* is the total number of available electrode sites, *k* is the number of sites to be selected, and x_i are the (zero/one) elements of the *n*-dimensional vector *x*. The elements of the matrix $T = (T_{ij})$ are the *T*-index values calculated from STL_{max} values from electrodes sites *i* and *j* ($j \neq i$), and *i* over the space of all available electrodes at time *t*. If the constraint is included in the objective function $f(x) = x^t Tx$ by introducing the penalty $\mu = \sum_{j=1}^{n} \sum_{i=1}^{n} |T_{ij}| + 1$, the optimization problem becomes equivalent to an unconstrained global optimization problem:

$$\min \left[x^t T x + \mu \left(\sum_{i=1}^{n} x_i - k \right)^2 \right],$$

where $x \in \{0, 1\}^n$. An electrode site *i* is selected if in the solution *x* to this problem $x_i = 1$. The selected *k* sites at time *t* then form the optimal or critical set of electrode sites to follow their dynamical entrainment forward in time for seizure prediction purposes. For robustness purposes, more than one set of *k*-sites (*k*-tuple) are followed forward in time. Typically the number of the next to the optimal *k*-tuples followed (denoted by *l*) may vary from 1 to 10. Both *k* and *l* parameters are estimated off-line from the testing portion of the available EEG data per rat through receiver operator curve (ROC; sensitivity/specificity) analysis (see[67] and the Results section below).

At the initiation of the seizure prediction program, which is a special case, sites had to be selected and monitored over time until the issue of the first warning. Instead of starting the program at a random time point, we here followed our previously published methodology.[63] That is, the first sites to be followed over time were derived from the preictal period of the first observed seizure in the data, according to the optimization methodology above, but with the additional constraint that the selected sites should be desynchronized in the immediate

postictal period (within 10 minutes after the end of that seizure). These initialization criteria secure that: (a) we follow forward in time sites relevant to the ictogenesis (they are synchronized before a seizure), and (b) these sites also are reset after that seizure, automatically becoming potentially sensitive precursors for a relapse to synchronization before the next seizure and facilitate the issue of a timely seizure warning, if the mechanism of ictogenesis is common across seizures in the same subject. After the first seizure, the prediction program started to run and issue seizure warnings, with electrode sites being adaptively reselected at each issued warning according to the following criteria: (a) the selected tuples of sites have *T*-indices less than the synchronization threshold T_{th} in the 10-minute window prior to a warning (i.e., synchronized sites immediately before a warning), and (b) sites should also be desynchronized in the 20 to 10-minute interval prior to the warning (i.e., sites desynchronized long before a warning). These two constraints for reselection of electrode sites at a warning were imposed to capture a progressive (not an abrupt) synchronization of the selected sites before a warning. After each warning, the *T*-indices of the newly selected electrode sites are followed forward in time and the conditions (see above) for the next seizure warning are applied. This site reselection process is repeated at every such detected dynamical transition (warning).

2.6. Automated just-in-time (JIT) stimulation control

Custom software (ESWP — Epileptic Seizure Warning Program) was developed in collaboration with EEGsoft Inc. to achieve data analysis in real time. The ESWP software was developed on a .NET framework to operate in a Windows based environment.

The necessary algorithms for seizure prediction included the following previously described methods:

- reconstruction of a 10.24 sec EEG data segment in the state space at time *t*
- calculation of the $STL_{\max}$ per EEG data segment and available electrode site at time *t*
- calculation of the *T*-index matrix within (*t*, *t* + 10 min) running windows over the $STL_{\max}$ profiles
- selection of the *l* (optimal and suboptimal) tuples of electrode sites (*k* sites per tuple)
- evaluation of the *T*-index per selected tuple of critical sites forward in time
- issue of seizure warnings based on the behavior of the monitored *T*-index of the selected tuples of the critical sites (see subsection above)

The ESWP software is capable of analyzing, plotting, and writing faster than real time to file the results of the analysis of more than 32-channels of EEG data.

A link to a custom-developed stimulator program was made with the ESWP software. The stimulator program was developed to trigger an A-M Systems Model 2300 stimulator unit (Calsborg, WA) and provide a stimulus, with predetermined pulse width, frequency and duration, to the stimulation electrodes at the time points that ESWP issues seizure warnings. Upon the issue of a seizure warning, the stimulator program was called as a function within the ESWP program and triggered the stimulator to generate a stimulus train of pulses of 1 minute in duration. The steps in the combined automated seizure prediction with deep brain electrical stimulation are depicted in the flow chart of Fig. 3. Initial selection of critical sites was made by ESWP upon the observation of a seizure from the EEG/video by the EEG technician in the Lab (ESWP started to run at that time point on the EEG — because it is faster than real time, it was able to catch up with the real time EEG recording within

minutes). Subsequently, reselection of the critical sites was automatically performed by ESWP 11 minutes after each issued warning/stimulus to allow no interference between this process and the produced stimulus artifact on the recorded EEG (see Fig. 2).

2.7. Experimental design

Testing of the automated seizure prediction and control system was carried out over 6 phases (Phase 0 to 5) following surgical implantation of electrodes in the rats who survived the epileptogenesis procedure. The functions performed within each phase are described below:

Phase 0—Search for optimal stimulus parameters based on resetting of brain dynamics. During this period, we conducted a search over the amplitude and frequency of a predetermined (and widely used in the literature) form of stimulus (train of square pulses of zero mean value and duration of 1 minute) using as criterion its capability to reset synchronized brain sites after its delivery.

Phase 1—Baseline EEG Recording (Seizures frequency/duration — Testing of ESWP prediction algorithm). Baseline EEG recording was performed to evaluate the frequency and duration of seizures occurring spontaneously in each rat. The presence of seizure activity was recorded by visual inspection of the EEG. During this period, evaluation of the performance of the seizure prediction scheme with respect to its sensitivity and specificity was also conducted. From this analysis, the parameters of upper threshold UT, tuple size k, and number of tuples l were chosen. This process allowed the prediction algorithm to be tailored per rat and parameters to be selected with a balance of sensitivity and specificity in seizure prediction (see Results section).

Phase 2—Automated Seizure Prediction combined with JIT Deep Brain Stimulation. (A closed-loop seizure control scheme.) During this phase of the experiment the ESWP software was programmed to deliver a one-minute stimulation train to the centromedial thalamic nucleus electrodes at seizure warnings. The frequency of seizure warnings and delivered stimulations were recorded. From the above, it is clear that stimulation is triggered at each issued seizure warning by ESWP in phase 2. If we stimulated at a warning and then did nothing for the next 2 hours (seizure prediction horizon for the ESWP), ignoring possibly issued subsequent seizure warnings in this interval, it would be like we were ignoring the indication each warning offers, that is, that the brain remained synchronized at those additional time points despite our stimulation at the first warning. There is no meaning of retrospectively evaluating the seizure prediction algorithm in phase 2 (and somehow use a seizure prediction horizon) because we intervene via stimulus and change the probability of a seizure occurrence all the time. There is no meaning in estimating true positive or false positive predictions in phase 2 and relate them to the ones in phase 1.

Phase 3—Post-JIT EEG Recording. Following the automated JIT stimulation control phase, at least one week recording with no stimulation was allowed to study a) the long-term effect (plasticity) of JIT stimulation on the frequency of seizures, and b) monitor when seizure frequency returns to the baseline values (phase 1) in order to start the periodic brain stimulation.

Phase 4—Periodic (P) Deep Brain Stimulation. (An open-loop seizure control scheme.) During this phase, periodic stimulation with identical stimulation parameters as the ones used in the automated JIT stimulation (phase 2), that is, one-minute stimulus pulse trains were delivered across the centromedial thalamic nucleus electrodes per rat. The period of stimulation was selected to be identical to the average inter-stimulus interval of JIT. Thus,

each rat received the same amount of stimulus in phases 2 and 4 but at different times. This phase was designed to investigate the effect of timing of stimulation on seizure frequency, and compare the performance of periodic versus timely deep brain stimulation on seizure control using the same subjects as controls of themselves.

Phase 5—Post-P EEG Recording. Following the periodic stimulation phase, a one week recording with no stimulation was performed to be used as the post-periodic stimulus control phase.

Per epileptic rat, phase 0 lasted for 1 week, while each of the subsequent phases lasted for at least seven days. A total of 6 rats were tested through the experimental phases with the number of days in each phase as shown in Table 1. Of note, Rat 1 died on Day 4 into Phase 4, and Rat 6 lost its recording hardware 1 day into Phase 5 and had to be sacrificed. The frequency and duration of seizures occurring in each of these phases were visually determined and recorded by the attending technician off-line.

3. Results

3.1. Resetting of brain dynamics by stimulation (Phase 0)

In phase 0, per rat, an extensive search over the parameters of the electrical stimulus (amplitude and frequency) for resetting of previously entrained (critical) tuples of brain sites was conducted. Resetting of brain dynamics by a high frequency (130–200 Hz) stimulus pulse was tested over a short range of stimulus amplitudes (100–600 μA, that is up to well below the 30-μC/cm^2 charge density limit for non-damaging stimulation in neural tissues given the size of our stimulating electrodes). The stimulus was administered for 1 minute, its pulse-width was kept constant at 100 μsec, and was delivered in a charge-balanced bipolar cathodic form across the centromedial thalamic electrodes. The optimal parameters are given in Table 2. We then used these optimal parameters of the electrical stimulus in phase 2 and 4 for control of seizures per rat over days under either of the two seizure control schemes (open or closed-loop) respectively.

3.2. Seizure prediction (Phase 1)

The performance of the seizure prediction algorithm was evaluated in phase 1 by a statistical analysis in terms of receiver operator curves (ROC), that is, estimation of sensitivities and specificities in terms of the parameters involved in the algorithm. Details of this method have been previously described.[67] In order to evaluate the accuracy of seizure warnings in terms of sensitivity and specificity, a prediction horizon is used. The seizure prediction horizon is defined as a window of time following a seizure warning during which the animal is likely to have a seizure. A warning is considered correct (true prediction) if a seizure occurs within the seizure prediction horizon; conversely if no seizure occurs, the warning is considered a false warning or false prediction. The unit of specificity used herein inversely corresponds to the number of false predictions per hour (total number of false predictions divided by the total number of hours of EEG analyzed).

In this study, the following parameters were varied to find the effect of each one on the seizure prediction scheme:

- upper threshold UT was varied from 3.5 to 5.0 in increments of 0.5
- tuple size k was varied from 2 to 5
- number of tuples l was varied from 1 to 5

For each of the parameter set tested, the seizure prediction horizon was fixed at 120 minutes, and all seizure warnings occurring within this prediction horizon were considered as a single warning. This ensures that there will be at most one true positive warning before a predicted seizure (thus sensitivity cannot be larger than 100%), but also may artificially decrease the false positive rate in the algorithm's evaluation period. The critical electrode sites for a parameter set were adaptively determined as described in Sec. 2.5 (see Fig. 1 for the result of one such set of parameters: $k = 3$, $l = 3$, UT = 5.0). In order to test the validity of the prediction scheme, the EEG datasets from phase 1 for each rat were split into training and testing datasets of equal duration (Table 1). Off-line determination of predicted seizures (sensitivity) and false positives (specificity) led to determination of the sensitivity and specificity per parameter set. The best parameter set was determined as the one that led to the best sensitivity (typically greater than 60%) and with the best corresponding specificity (typically less than 0.2 false predictions per hour) in the training dataset. If more than one parameter set fit within these limits, the set with the highest sensitivity was chosen for evaluation of ESWP in the testing dataset.

A combined total of 747 seizures were recorded across six epileptic rats over a collective duration of nearly 52 days of EEG recording in this phase (see Table 3). Seizures were recorded by visual inspection of the EEG and without knowledge of the results from the dynamical analysis. Seizures were typically complex partial with secondary generalization. Seizure activity in the EEG was usually apparent first in the deep electrodes, was associated with hippocampal or thalamic fast activity subsequently spreading to cortical areas, which showed characteristic spike and wave EEG patterns. Propagation of the EEG signal was apparent within the seizure. The end of the seizures was typically abrupt and showed a suppression of the EEG with low amplitude slowing. When secondary generalization was present, almost all seizures could be classified as a Racine Level 5 seizure with rearing and loss of balance.

In the training datasets, the full ROC analysis of the prediction scheme was performed in terms of sensitivity and specificity values for UT, k, and l. For the testing datasets, the optimal upper threshold, tuple size, and number of tuples were chosen from the ROC analysis of the training datasets specific for each rat. The thus determined optimal sets of parameters per rat are given in the first 3 columns of Table 4. Also in this table, the attained sensitivity, specificity and mean prediction time by running the ESWP with these optimal parameters are given per rat. Note that sensitivity and specificity analysis was performed in predicting seizures subsequent to the first one (retrospective analysis). Overall sensitivity of EWSP across rats was 0.66 (251/381), false positives rate 0.1 per hour, and mean prediction time (time of true warning before a seizure) 55 minutes.

The prediction algorithm ESWP was then run, with the optimal parameters determined from the EEG training datasets (phase 1), on the EEG testing datasets (phase 1) per rat. The sensitivity and specificity analysis in predicting seizures (including the first one — prospective analysis) was then performed on the testing datasets. The results are shown in Table 5. Overall sensitivity of EWSP across rats here was 0.746 (264/354), false positives rate 0.16 per hour, and mean prediction time (time of true warning before a seizure) 64 minutes. It is worthy to compare the performance of EWSP in high versus low seizure frequency datasets. Rat 3 had only 4 seizures in 83.3 hours (training dataset), 7 seizures in 83.3 hours (testing dataset) (see Table 3). EWSP's sensitivity in the training dataset of this rat was 0.667 with 0.036 false predictions per hour (see Table 4), that is, very small compared to the ones of Rats 1 and 2 which had at least 5 times shorter interseizure intervals. In the testing dataset of this rat (see Table 5) EWSP's sensitivity was 0.833 (very much comparable to the one in Rats 1 and 2) with 0.036 false predictions per hour (the smallest number of all rats). In light of these observations, an implication that our 2 hour

prediction horizon makes any issued warning a true prediction is not withstanding due to the actual variability and clustering of seizures in a rat. If that were true, in the example given above, the prediction algorithm should perform much better in Rats 1 and 2 than in Rat 3, which is not the case.

3.3. Just-in-time seizure control (Phase 2)

One-minute pulses of stimulus were delivered to the thalamic electrodes at all seizure warnings issued by ESWP. The rest of stimulus parameters per rat were as in Table 2. The prediction parameters used per rat were the ones derived in phase 1 (see Table 4). The resulted average of inter-stimulus intervals is given per rat in Table 6. (This average was subsequently used as the period of stimulation in the periodic stimulation scheme.)

The performance of seizure control via JIT stimulation per rat is given in Table 7. It can be evaluated by comparing the mean seizure frequency per day and seizures' duration during phase 2, to the ones in the baseline (phase 1), as well as to the ones after the end of JIT seizure control (phase 3). Details of its performance for Rat 2 are given in Fig. 4(a). Statistical comparisons of seizure frequency were performed via a Wilcoxon sign-ranked test with a significance level of $p < 0.05$. Five of six rats showed a reduction in mean seizure frequency per day when compared to baseline seizure levels, with two of the rats (Rat 2 and 6) showing a significant reduction of more than 50%. Rat 2, which had a significant reduction in seizure frequency during the JIT control, after the end of all phases of the experiment, was engaged to a repetition of phase 1 and 2 in an attempt to verify one more time the previously observed reduction of seizure frequency, and it was again found to be significant (see entry Rat 2** in the third row of Table 7). Increase of seizure frequency after the end of JIT, in phase 3, was also observed. For Rat 2, the change of seizure frequency in phases 1, 2 and 3 of the experiment are shown in Fig. 4 through Tukey's box-and-whisker plots. Changes in seizure duration were compared using the Kolmogorov Smirnov Z-test and are also shown in Table 7 with significance set at $p < 0.01$. Three of the rats (Rat 1, 3 and 6) showed no significant changes in seizure duration at JIT stimulation period, two of them showed significant decrease (Rat 4 and 5) and one of them (Rat 2) a small but significant increase in the duration of their seizures. To better visualize such seizure frequency reduction results in combination with the results from seizure duration, in the last two columns of Table 7 we present the estimated average time a rat spends seizing (ATS) per day under JIT and at its baseline. It is important to note that, under JIT, there was about 2 to 3 times reduction of ATS in 4 of the 6 rats in the study.

3.4. Periodic seizure control (Phase 4)

Periodic stimulation was performed (phase 4), following a baseline rest period (phase 3). The stimulus given was identical to the one in JIT but repeated periodically with a period equal to the mean value of JIT's interstimulus interval of phase 2 (see Table 6) per rat.

The performance of seizure control via periodic stimulation per rat is given in Table 8. It was evaluated in terms of the same criteria as JIT. Details of its performance for Rat 2 are given in Fig. 4(b). Statistical comparisons of seizure frequency were performed via a Wilcoxon sign-ranked test with a significance level of $p < 0.05$. Only three rats (Rat 1, 5, 6) showed a reduction in seizure frequency during periodic control. Only one of them showed a significant decrease of seizure frequency (Rat 6). Therefore, Rat 6 was the only rat that showed a significant decrease in seizure frequency with either control scheme utilized. The rest of the rats (Rat 2, 3, 4) showed an increase in seizure frequency, with one of them (Rat 4) showing a significant increase. For Rat 2, the change of seizure frequency in phases 1, 2 and 3 of the experiment are shown in Fig. 5 through box-and-whisker plots. Changes in seizure duration were compared using the Kolmogorov Smirnov *Z*-test and are also shown in

Table 8 with significance set at $p < 0.01$. Two of the rats (Rat 3 and 5) showed no significant changes in seizure duration during periodic stimulation, two of them showed significant decrease (Rat 2 and 4) and two of them (Rat 1 and 6) significant increase in the duration of their seizures. To better visualize any seizure frequency reduction results in combination with the results from seizure duration, in the last two columns of Table 8 we present the estimated average time a rat spends seizing (ATS) per day under P and at its corresponding baseline. It is important to note that, under P, there was about 2 times reduction of ATS in only 1 of the 6 rats in the study. In addition, in Fig. 5, for one rat (Rat 2) we have included the variation of daily seizure frequency over time for JIT and its baseline (top panel), and for P and its baseline (middle panel). Because in this rat we attempted a repetition of the whole experiment (denoted Rat 2*), these additional data for JIT (phase 2*) and its second baseline (phase 1*) are also depicted (bottom panel). From this figure it is clear that the periodic (P) stimulation started from a very similar baseline (with respect to pre-existing seizure frequency) to the one of JIT stimulation. This was typical in all our rats in the study. Therefore, the observed big differences in performance between JIT and P cannot easily be justified by the observed small differences between their baselines. A final observation from Fig. 5 is that JIT seems to be pretty robust: it seems to be equally effective in seizure frequency reduction during phase 2 or 2* (compare Figs. 5(a) and 5(c)), that is, irrespectively of these phases being weeks apart and the in-between application of the periodic stimulation.

3.5. Brain dynamics of seizure control

In order to investigate possible causes for the observed successes/failures of seizure control, a comparative analysis of dynamical synchronization and seizure frequency during both JIT and periodic control phases was performed. Per rat, in phases 2 and 4, we first estimated the global brain synchronization via a global *T*-index (average of *T*-indices of all pairs of available electrode sites within 2-hour non-overlapping running windows) over time. We then compared the resulting global *T*-index curve with the one generated from the number of seizures that occurred within the corresponding windows over time.

Such a comparison over time is shown in Fig. 6(a) for Rat 2 in phase 2 (JIT stimulation period). From this figure it is evident that: (a) when seizure frequency was significantly decreased during the JIT stimulation (e.g., in days 2 and 3 to almost zero), *T*-index assumed its highest values, denoting significant desynchronization of brain dynamics and (b) when seizure frequency was high, *T*-index assumed low values, denoting synchronization of brain dynamics. We went one step further and estimated the cross-correlation coefficient between the two curves in Fig. 6. The value of this coefficient across the whole record was -0.72 at $p < 0.001$. Even when we correlated the curves in the second half of the record only, the cross-correlation coefficient was statistically significant negative (-0.20 at $p < 0.02$). This result means that the global *T*-index is significantly and inversely correlated with the seizure frequency, and therefore desynchronization of brain dynamics significantly correlates with seizure control. In Fig. 6(b), we show the actual JIT stimulation rate (number of stimuli per 2 hour running windows) over time for this rat in this period. It shows that stimulation was on across all days in phase 2, and therefore we cannot base the failure of maintaining seizure control after day 4 on lack of stimulation. However, taking also in consideration the results from Fig. 6(a), we can say that lack of seizure control was most probably due to inability of the stimulation to reset the brain. Because high *T*-index values reflect desynchronized brain dynamics, which may be due to either the effect of the stimulation or the seizures (either of the two do reset the brain, as we have shown herein — see Figs. 1 and 2 — and in the past). However, in the framework of this experiment, stimulation is designed to be ON (via the seizure prediction program) before a seizure occurs. If stimulation is ineffective in resetting the brain and stop the route of the brain towards a seizure, the seizure will occur. In this

case, stimulation rate will be high and seizure rate will be high, while *T*-index will be low (right portions of Figs. 6(a) and 6(b)). However, if stimulation is effective, *T*-index will be relatively high, stimulation rate will again be high and seizure rate will be low (left portions of Figs. 6(a) and 6(b)).

Across rats, Fig. 7 cumulatively shows the same result. In this figure, we plot the global *T*-index values (distributed in box-and-whisker boxes) estimated from every 2 hour non-overlapping EEG segment in phase 2 versus the number of seizures occurred in that same EEG segment. That is, if 0 seizures occurred in an EEG segment, the *T*-index estimated from that segment would be placed in the first box in a panel of Fig. 7, etc. Also, this means that one box-and-whisker box of *T*-index corresponds to one value of seizure frequency measured by number of seizures per 2 hours. We observe that Rats 2 and 6 (i.e. the ones that responded to JIT with a significant seizure frequency reduction) exhibit significantly high values of *T*-index, and hence desynchronization of brain dynamics, when seizures do not occur often (low seizure frequency; for example 0 or 1 seizure per 2 hours). On the contrary, when seizures occur often (high seizure frequency values; for example 2 to 7 per 2 hours), the *T*-index values are low, denoting synchronization of brain dynamics. It is interesting to note that Rat 3, which exhibited a large (−63.69%) but not a significant reduction in its seizure frequency (see Table 7), also shows the above inverse and monotonous relation between desynchronization of brain dynamics and seizure frequency. It is also interesting to note that, in all other rats (Rat 1, 4, 5) where JIT failed to significantly reduce their seizures, no inverse relation between desynchronization and seizure frequency can be observed. In this case, *T*-index values remain low (synchronized brain sites) and relatively constant in terms of seizure frequency.

During the periodic stimulation (phase 4), lack of reduction of seizure frequency across rats corresponded well with the lack of desynchronization of their brain dynamics too. Figure 8 clearly shows this result in Rat 2. Synchronization of brain dynamics remained high (low global *T*-index value) across the whole period of periodic stimulation and seizures persisted. It is noteworthy that, even in this case of failure of seizure control, seizure frequency was anti-correlated with *T*-index (e.g. local maxima of *T*-index correspond to local minima of seizure frequency). Calculating the cross-correlation coefficient between the seizure frequency and the global *T*-index curves gives a significant ($p < 0.05$) value of −0.12. This result again means that the global *T*-index is significantly and inversely correlated with the seizure frequency, and therefore it seems that, even in this case, desynchronization of brain dynamics significantly correlates with seizure control.

4. Discussion

In this study a stand-alone closed-loop automated seizure prediction and just-in-time stimulation control system was developed that utilizes methods from nonlinear dynamics coupled with deep brain stimulation techniques. The automated JIT stimulation control system was implemented in six chronically epileptic rats. The performance of the automated system in controlling seizures was compared to an open-loop periodic stimulation control scheme with identical stimulus characteristics and period of stimulation equal to the JIT's mean of inter-stimulus intervals per rat. Since this was a within-subject comparison study of methods for seizure control, the unambiguous localization of the stimulation electrodes in the centromedian thalamic nucleus is not a factor on the conclusions reached by the study.

Sensitivity for prediction of seizures by the ESWP algorithm (an integral part of the JIT system in this investigation) in the testing datasets was higher than 80% for every rat with the exception of Rat 6 (slightly less than 50% — see Table 5). The average prediction time (time from an issue of a true warning by ESWP to the impending seizure occurrence) across

rats in the testing datasets was 63.7 minutes. The average specificity of ESWP for seizure prediction in the testing datasets across rats was 0.164 false warnings per hour, or else about 3 false warnings per 20 hours. Overall, across rats in the testing datasets, true warnings were issued in 264 out of 354 seizures yielding a mean sensitivity of 74.6% and 101 false warnings over 617 hours of recording giving 0.164 false warnings per hour (about 3 false warnings every 19 hours).

In this animal model, despite the above performance of ESWP, the automated JIT stimulation control scheme was significantly effective only in 33% of the rats tested with respect to seizure frequency (although 83% of them did experience a reduction in seizure frequency), and had mixed (mostly non-significant) results with respect to seizure duration (see Table 7). This performance was however a substantial improvement over the one of periodic control scheme, which resulted to an increased seizure frequency in 50% of the rats tested, and a significant reduction of seizure frequency in 17% of them. It appears that timing of stimulation is a very important factor for achievement of seizure control. These results suggest that the automated seizure control scheme may provide a more effective means of seizure control than the periodic one.

In terms of brain dynamics, it was found that successful seizure control was highly correlated with the ability of JIT or periodic stimulation to reset dynamically synchronized brain sites, whereas unsuccessful seizure control was correlated with the failure of stimulation to desynchronize the brain. Interestingly, based on an assumption of desynchronization of dynamics prior to seizures,[68] it was recently attempted to show that DBS may have to be designed to "synchronize the epileptic brain in order to prevent seizures". This attempt was not successful, producing mixed results.[69] The results from our current study suggest that the key for prevention of seizures through stimulation is the desynchronization of the synchronized epileptic brain (resetting). This conjecture is in agreement with Duran *et al.*[70] and our theory of synchronization of dynamics as precursor to seizures, and of seizures as the natural means of the brain to reset.[22,23,48] Our long-term continuous EEG studies on status epilepticus (SE)[23,71] also support this conjecture (successful AED intervention desynchronizes the synchronized SE brain, despite claims for the opposite in analogous investigations in SE[72]). Conduct of larger scale studies to shed more light on these important conjectures for epileptogenesis, ictogenesis and the treatment of epilepsy is contemplated.

There are other factors that may have influenced the performance of the stimulation systems investigated in this study. The form of the stimulus was common in both open and closed-loop systems and consistent with ones currently in wide use. However, as Fig. 2 clearly shows, the form of the stimulus may influence the desynchronization of the dynamics of the brain only for a limited time (e.g., no more than 30 minutes in the case presented). Along these lines, novel forms of stimulus have recently been proposed for closed-loop stimulation systems,[24,25] have produced promising results in simulation studies with biologically plausible models of components of the epileptic brain,[26–28] and therefore may prove to be more effective than the ones in current practice for seizure control.

Another factor that needs further investigation is the optimal location of the stimulation electrodes. In this study, the stimulation electrodes were placed in the centromedial thalamic nucleus. As we described in the introduction, many groups have tried stimulating different areas of the brain (e.g. anterior thalamic nucleus). Where to stimulate more effectively is certainly still an open question. Therefore, the field of neuromodulation/neurostimulation may well benefit from advances in precise localization of the epileptogenic focus.[73–74]

Our last, but not least, observation from this study has to do with the long-term effect of stimulation on seizure frequency. For example, it is clear from Fig. 6(a) that JIT control may lose efficacy over days. This could be due to any of the following factors that need to be separately or in conjunction investigated further. First, brain tissue reacts with the long-term implantation of the recording and/or stimulating electrodes and renders them dysfunctional. However, there is an indication that that was not the case here, as the repetition of experiment in Rat 2** shows (seizure control was demonstrated via JIT weeks after phase 2 in this rat). Second, the employed ESWP seizure prediction algorithm becomes over time less sensitive to the impending seizures under the influence of stimulation-imposed changes in the brain dynamics. This is possible and may require the development of better adaptive algorithms than the existing one to monitor the dynamics of the brain. Second generation ESWP algorithms are being developed along these lines by our group, with the additional advantage of no need of a training process for the identification of the optimal ESWP parameters. Third, there may be a need to change the form of the stimulus itself over time, according to the change of the brain dynamics, for it to continue to be effective in seizure control in the long-term. Investigations along these lines have been performed and show the importance of this factor for seizure control.[24–28] Fourth, location of stimulation may need to change over time. This might be necessary to be performed if synchronization of dynamics moves over time to different brain locations. An alternative method might be to stimulate at a central location with good access to all (or most of) the critical electrode sites in each case.

5. Conclusion

In this small-scale, real-time, in-vivo DBS study with epileptic rodents, we have shown that the development of an effective closed-loop seizure control system, that has the recorded EEG as input and electrical stimulation as output, is feasible and promising. Such a system, employing the concept of JIT (just in time) electrical stimulation, can be more effective than a corresponding open-loop periodic stimulation system that consumes the same amount of battery energy. It also appears that the concept of brain's dynamical desynchronization or resetting is central to the success of a seizure control system. Finally, the form of stimulus itself and its effect on seizure control may be one of the missing pieces of the puzzle for a highly efficacious long-term seizure control. For example, pulse stimuli (like the ones used in this study and advocated widely in the literature) may not abate every upcoming seizure *even if they are JIT delivered*, as it is shown in this study as well as in mathematical models of epilepsy (periodic stimulation widely underperforms there too).[18–20]

In summary, this study, as the first-stage of work in progress, shows that it is feasible to close the loop between seizure prediction and deep brain stimulation for a better control of seizures, and we believe it also contributes fundamentally to the understanding and interpretation of the successes and failures of current and future seizure control schemes. Therefore, studies of a larger scale along these lines are contemplated.

Acknowledgments

We would like to thank Victor Baidoon and Alexander Drachev of EEGsoft Inc. for their effort to make the JIT system operate in real-time. We would also like to thank the 7 anonymous reviewers for their constructive comments and suggestions. Support for this study has been provided in part by the National Institute of Health EB002089 BRP grant on Brain Dynamics, the Barrow Neurological Foundation, the Epilepsy Research Foundation of America and Ali Paris Fund for LKS Research, the National Science Foundation grant No. 0601740, and the Science Foundation Arizona (Competitive Advantage Award CAA 0281-08).

References

1. Kwan P, Brodie MJ. Early identification of refractory epilepsy. N Engl J Med. 2000; 342(5):314–319. [PubMed: 10660394]
2. Fisher RS, Handforth A. Reassessment: Vagus nerve stimulation for epilepsy: A report of the Therapeutics and Technology Assessment subcommittee of the american academy of neurology. Neurology. 1999; 53(4):666–669. [PubMed: 10489023]
3. Hodaie M, et al. Chronic anterior thalamus stimulation for intractable epilepsy. Epilepsia. 2002; 43(6):603–608. [PubMed: 12060019]
4. Kerrigan JF, et al. Electrical stimulation of the anterior nucleus of the thalamus for the treatment of intractable epilepsy. Epilepsia. 2004; 45(4):346–354. [PubMed: 15030497]
5. Velasco M, et al. Acute and chronic electrical stimulation of the centromedian thalamic nucleus: Modulation of reticulo-cortical systems and predictor factors for generalized seizure control. Arch Med Res. 2000; 31(3):304–315. [PubMed: 11036182]
6. Yamamoto J, et al. Low-frequency electric cortical stimulation has an inhibitory effect on epileptic focus in mesial temporal lobe epilepsy. Epilepsia. 2002; 43(5):491–495. [PubMed: 12027909]
7. Chkhenkeli SA, et al. Electrophysiological effects and clinical results of direct brain stimulation for intractable epilepsy. Clin Neurol Neurosurg. 2004; 106(4):318–329. [PubMed: 15297008]
8. Bragin A, Wilson CL, Engel J Jr. Rate of interictal events and spontaneous seizures in epileptic rats after electrical stimulation of hippocampus and its afferents. Epilepsia. 2002; 43(Suppl 5):81–85. [PubMed: 12121300]
9. Velasco AL, et al. Electrical stimulation of the hippocampal epileptic foci for seizure control: A double-blind, long-term follow-up study. Epilepsia. 2007; 48(10):1895–1903. [PubMed: 17634064]
10. Boon P, et al. Deep brain stimulation in patients with refractory temporal lobe epilepsy. Epilepsia. 2007; 48(8):1551–1560. [PubMed: 17726798]
11. Cuellar-Herrera M, et al. Evaluation of GABA system and cell damage in parahippocampus of patients with temporal lobe epilepsy showing antiepileptic effects alter subacute electrical stimulation. Epilepsia. 2004; 45:459–466. [PubMed: 15101827]
12. Velasco AL, et al. Subacute and chronic electrical stimulation of the hippocampus on intractable temporal lobe seizures. Arch Med Res. 2000; 31:316–328. [PubMed: 11036183]
13. Velasco F, Velasco M, Jimenez F. Predictors in the treatment of difficult to control seizures by electrical stimulation of the centromedian thalamic nucleus. Neurosurgery. 2000; 47:295–305. [PubMed: 10942002]
14. Lado FA, Velisek L, Moshe SL. The effect of electrical stimulation of the subthalamic nucleus on seizures is frequency dependent. Epilepsia. 2003; 44(2):157–164. [PubMed: 12558568]
15. Mirski MA, et al. Anticonvulsant effect of anterior thalamic high frequency electrical stimulation in the rat. Epilepsy Res. 1997; 28(2):89–100. [PubMed: 9267773]
16. Nail-Boucherie K, et al. Suppression of absence seizures by electrical and pharmacological activation of the caudal superior colliculus in a genetic model of absence epilepsy in the rat. Exp Neurol. 2002; 177(2):503–514. [PubMed: 12429195]
17. Velisek L, Veliskova J, Moshe SL. Electrical stimulation of substantia nigra pars reticulata is anticonvulsant in adult and young male rats. Exp Neurol. 2002; 173(1):145–152. [PubMed: 11771947]
18. Vercueil L, et al. High-frequency stimulation of the subthalamic nucleus suppresses absence seizures in the rat: Comparison with neurotoxic lesions. Epilepsy Res. 1998; 31(1):39–46. [PubMed: 9696299]
19. Osorio I, et al. High frequency thalamic stimulation for inoperable mesial temporal lobe epilepsy. Epilepsia. 2007; 48(8):1561–1571. [PubMed: 17386053]
20. Osorio I, et al. Automated seizure abatement in humans using electrical stimulation. Ann Neurol. 2005; 57(2):258–268. [PubMed: 15668970]
21. Kossoff EH, et al. Effect of an external responsive neurostimulator on seizures and electrographic discharges during subdural electrode monitoring. Epilepsia. 2004; 45(12):1560–1567. [PubMed: 15571514]

22. Iasemidis LD. Epileptic seizure prediction and control. IEEE Trans Biomed Eng. 2003; 50(5):549–558. [PubMed: 12769431]
23. Iasemidis, LD., et al. A new look into epilepsy as a dynamical disorder: Seizure prediction, resetting and control. In: Schwartzkroin, Philip, editor. Encyclopedia of Basic Epilepsy Research. Elsevier; Oxford: in press
24. Tsakalis KS, Iasemidis LD. Control aspects of a theoretical model for epileptic seizures. Int J Bifurcation and Chaos. 2006; 16(7):2013–2027.
25. Tsakalis KS, et al. A feedback control systems view of epileptic seizures. Cybernetics Systems Analysis. 2006; 42:483–495.
26. Chakravarthy N, et al. Modeling and controlling synchronization in a neuron-level population model. Int J Neural Systems. 2007; 17:123–138.
27. Chakravarthy N, et al. Controlling epileptic seizures in a neural mass model. J Combinatorial Optimization. 2009; 17:98–116.
28. Tsakalis KS, et al. Homeostasis of brain dynamics in epilepsy: A feedback control systems perspective of seizures. Annals of Biomedical Engineering. in press.
29. Good, LB., et al. Automatic seizure prediction and deep brain stimulation control in epileptic rats. Philadelphia, Pennsylvania. American Epilepsy Society Annual meeting; 2007. Young Investigator Award
30. Good LB, et al. Seizure prediction in a rat model of chronic epilepsy. Epilepsia. 2006; 47(S4):305–306.
31. Good LB, et al. Nonlinear dynamical analysis of deep brain stimulation for control of epileptic seizures in rats. Epilepsia. 2006; 46:330.
32. Good, LB., et al. Real-time control of epileptic seizures. 3rd European Medical and Biological Engineering Conference (EMBEC); Prague. Nov 20–25; 2005. p. 6
33. Good, L. PhD Dissertation. Department of Bioengineering, Arizona State University; 2007. Automated seizure prediction and control in a rat model of chronic epilepsy.
34. Iasemidis LD, et al. Nonlinear dynamics of ECoG data in temporal lobe epilepsy. J Electroencephalography and Clinical Neurophysiology. 1988; 5:339.
35. Iasemidis, LD., et al. Linear and nonlinear modeling of ECoG in temporal lobe epilepsy. 25th Annual Rocky Mountain Bioengineering Symposium; 1988. p. 187-193.
36. Iasemidis LD, et al. Phase space topography of the electrocorticogram and the Lyapunov exponent in partial seizures. Brain Topogr. 1990; 2:187–201. [PubMed: 2116818]
37. Iasemidis, LD.; Principe, JC.; Sackellares, JC. Spatiotemporal dynamics of human epileptic seizures. In: Harrison, RG., et al., editors. 3rd Experimental Chaos Conference; World Scientific; 1996. p. 26-30.
38. Casdagli MC. Characterizing nonlinearity in invasive EEG recordings from temporal lobe epilepsy. Physica D. 1996; 99:381–399.
39. Iasemidis LD, Sackellares JC. Chaos theory and epilepsy. Neuroscientist. 1996; 2:118–126.
40. Iasemidis, LD., et al. Spatiotemporal transition to epileptic seizures: A nonlinear dynamical analysis of scalp and intracranial EEG recordings. In: FL, Silva; JC, Principe; LB, Almeida, editors. Spatiotemporal Models in Biological and Artificial Systems. IOS Press; 1997. p. 81-88.
41. Casdagli MC, et al. Nonlinearity in invasive EEG recordings from patients with temporal lobe epilepsy. Electroenceph Clin Neurophysiol. 1997; 102:98–105. [PubMed: 9060860]
42. Sackellares, JC., et al. Epilepsy — when chaos fails. In: Lehnertz, K., et al., editors. in Chaos in the Brain?. World Scientific; Singapore: 2000. p. 112-133.
43. Iasemidis, LD., et al. On the prediction of seizures, hysteresis and resetting of the epileptic brain: Insights from models of coupled chaotic oscillators. In: Bountis, T.; Pneumatikos, S., editors. Order and Chaos. Vol. 8. Publishing House of K Sfakianakis; 2003. p. 283-305.
44. Iasemidis, LD., et al. Prediction of epileptic seizures by linear and nonlinear methods. International Nonlinear Sciences Conference on Research and applications in the Life Sciences; Vienna, Austria. February 7–9, 2003;
45. Iasemidis LD, et al. Prediction of human epileptic seizures based on optimization and phase changes of brain electrical activity. J Optimization Methods and Software. 2003; 18:81–104.

46. Adeli H, Zhou Z, Dadmehr N. Analysis of EEG records in an epileptic patient using wavelet transform. J Neuroscience Methods. 2003; 123(1):69–87.
47. Ghosh-Dastidar S, Adeli H, Dadmehr N. Mixed-band wavelet-chaos-neural network methodology for epilepsy and epileptic seizure detection. IEEE Transactions on Biomedical Engineering. 2007; 54(9):1545–1551. [PubMed: 17867346]
48. Iasemidis LD, et al. Dynamical resetting of the human brain at epileptic seizures: Application of nonlinear dynamics and global optimization techniques. IEEE Trans Biomed Eng. 2004; 51(3): 493–506. [PubMed: 15000380]
49. Honchar MP, Olney JW, Sherman WR. Systemic cholinergic agents induce seizures and brain damage in lithium-treated rats. Science. 1983; 220(4594):323–325. [PubMed: 6301005]
50. Persinger MA, Makarec K, Bradley JC. Characteristics of limbic seizures evoked by peripheral injections of lithium and pilocarpine. Physiology & Behavior. 1988; 44(1):27–37. [PubMed: 2853377]
51. Leite JP, Cavalheiro EA. Effects of conventional antiepileptic drugs in a model of spontaneous recurrent seizures in rats. Epilepsy Research. 1995; 20(2):93–104. [PubMed: 7750514]
52. Mathern GW, et al. In contrast to kindled seizures, the frequency of spontaneous epilepsy in the limbic status model correlates with greater aberrant fascia dentata excitatory and inhibitory axon sprouting, and increased staining for N-methyl-D-aspartate, AMPA and GABA(A) receptors. Neuroscience. 1997; 77(4):1003–1019. [PubMed: 9130782]
53. Persinger MA, et al. Behaviors of rats with insidious, multifocal brain damage induced by seizures following single peripheral injections of lithium and pilocarpine. Physiology & Behavior. 1993; 53(5):849–866. [PubMed: 8511200]
54. Priel MR, dos Santos NF, Cavalheiro EA. Developmental aspects of the pilocarpine model of epilepsy. Epilepsy Res. 1996; 26(1):115–121. [PubMed: 8985693]
55. Turski L, et al. Review: Cholinergic mechanisms and epileptogenesis. The seizures induced by pilocarpine: A novel experimental model of intractable epilepsy. Synapse. 1989; 3(2):154–171. [PubMed: 2648633]
56. Racine RJ. Modification of seizure activity by electrical stimulation: II. Motor seizure. Electroencephalography and Clinical Neurophysiology. 1972; 32(3):281–294. [PubMed: 4110397]
57. Lopes da Silva, F. EEG analysis theory and practice; Computer-assisted EEG dianosis: Pattern recognition techniques. In: Niedermeyer, E.; Lopes da Silva, F., editors. Electroencephalography: Basic principles, clinical applications and related fields. Urban & Schwarzenburg; Baltimore: 1987. p. 971-919.
58. Abarbanel, HDI. Analysis of Observed Chaotic Data. Springer-Verlag; New York: 1996.
59. Takens, F. Detecting strange attractors in turbulence. In: Rand, DA.; Young, LS., editors. Dynamical systems adn turbulence, Lecture notes in mathematics. Springer-Verlag; Heidelburg: 1981.
60. Iasemidis, LD.; Principe, JC.; Sackellares, JC. Measurement and quantification of spatiotemporal dynamics of human epileptic seizures. In: Akay, M., editor. Nonlinear biomedical Signal Processing. IEEE Press; 2000. p. 294-318.
61. Iasemidis, LD.; Sackellares, JC. The temporal evolution of the largest Lyapunov exponent on the human epileptic cortex. In: Duke, DW.; Pritchard, WS., editors. Measuring chaos in the human brain. World Scientific; Singapore: 1991. p. 49-82.
62. Wolf A, et al. Determining Lyapunov exponents from a time series. Physica D. 1985; 16:285–317.
63. Iasemidis LD, et al. Adaptive epileptic seizure prediction system. IEEE Trans Biomed Eng. 2003; 50(5):616–627. [PubMed: 12769437]
64. Iasemidis LD, et al. Long-term prospective on-line real-time seizure prediction. J Clin Neurophysiol. 2005; 116:532–544.
65. Iasemidis LD, et al. Quadric binary programming and dynamical system approach to determine the predictability of epileptic seizures. Journal of Combinatorial Optimization. 2001; 5:9–26.
66. Chaovalitwongse W, et al. Dynamical approaches and multi-quadratic integer programming for seizure prediction. J Optimization Methods and Software. 2005; 20:383–394.

67. Shiau, DS., et al. Nonlinear dynamical and statistical approaches to investigate dynamical transitions before epileptic seizures. In: Pardalos, P., et al., editors. Quantitative Neuroscience. Kluwer Academic Publishers; 2004. p. 239-249.

68. Mormann F, et al. Epileptic seizures are preceded by a decrease in synchronization. Epilepsy Research. 2003; 53:173–185. [PubMed: 12694925]

69. Schindler K, Elger CE, Lehnertz K. Changes of EEG synchronization during low-frequency electric stimulation of the seizure onset zone. Epilepsy Research. 2007; 77(2):108–119. [PubMed: 17980557]

70. Durand DM, Warman EN. Desynchronization of epileptiform activity by extracellular current pulses in rat hippocampal slices. J Physiology. 1994; 480:527–537.

71. Good, LB., et al. Brain dynamical disentrainment by anti-epileptic drugs in rat and human status epilepticus. 26th IEEE EMBS Annual International Conference; Sept 1–4; San Francisco. 2004. p. 176-179.

72. Schindler K, Elger CE, Lehnertz K. Increasing synchronization may promote seizure termination: Evidence from status epilepticus. Clinical Neurophysiology. 2007; 118:1955–1968. [PubMed: 17644031]

73. Iasemidis LD, Sackellares JC, Williams WJ. Localizing preictal temporal lobe spike foci using phase space analysis. Electroencephalography and Clinical Neurophysiology. 1990; 75(1):63–64.

74. Sabesan S, et al. Information flow and application to epileptogenic focus localization from EEG. IEEE Trans Neural Systems. in press.

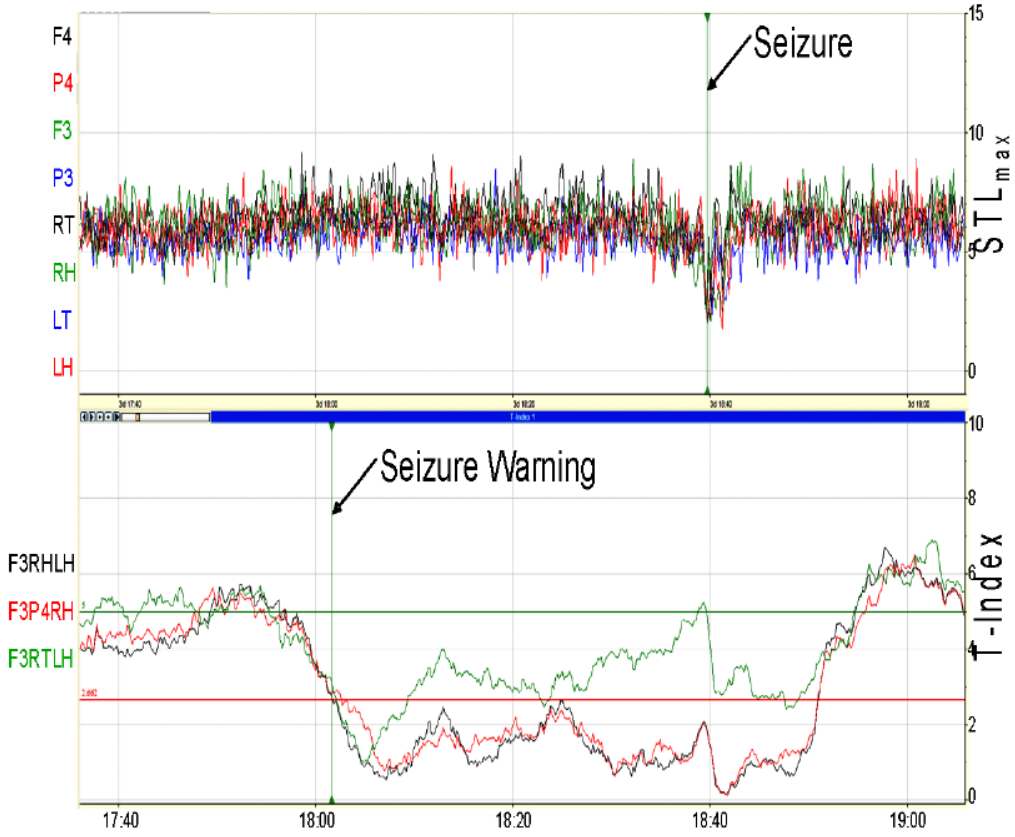

Fig. 1.

Dynamical transition into and out of a typical seizure in a rat (as it appears on the real-time ESWP screen). Top Panel: STL_{max} profiles estimated from a 90-minute EEG segment recorded from the right frontal (F4), right parietal (P4), left frontal (F3), left parietal (P3), right thalamic (RT), right hippocampal (RH), left thalamic (LT), and left hippocampal (LH) electrodes; units of STL_{max} are in bits/sec; seizure occurred 60 minutes into the recording (vertical line) and lasted for 3 minutes. Bottom Panel: *T*-index profiles of (F3, RH, LH), (F3, P4, RH), and (F3, RT, LH) tuples of electrode sites. The critical entrainment threshold (CT) with $\alpha = 0.01$ is shown by the red horizontal line at 2.662, and upper threshold (UT) is also shown at 5.0 by the green horizontal line. A seizure is noted at time 18:40 with a seizure warning elicited at 18:02 when there is a transition in the *T*-index from above the UT to below the CT.

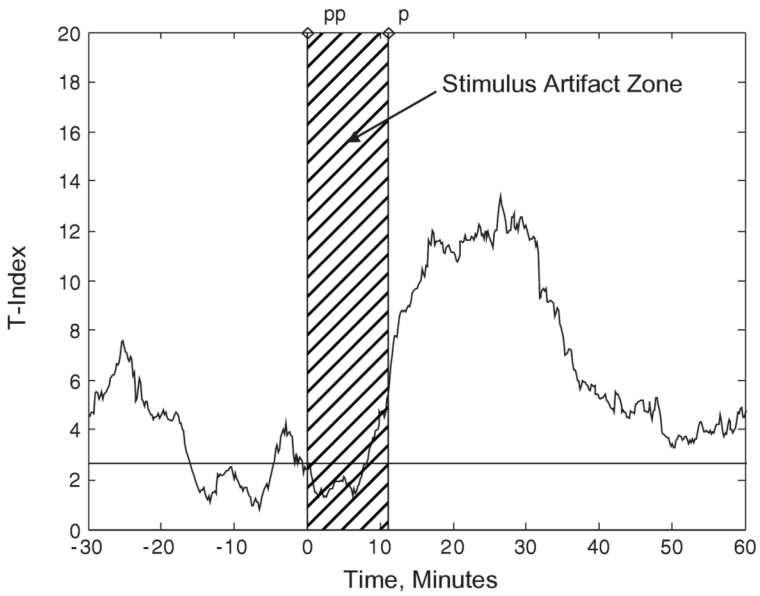

Fig. 2.

Desynchronization of synchronized brain dynamics by electrical stimulus in the brain of an epileptic rat. The stimulus train characteristics were: 1 minute duration, intensity of 200-μA, frequency of 130-Hz. It was applied at time zero at the left thalamic (LT2) and left hippocampal (LH) electrode pair in the brain of an epileptic rat. The stimulus artifact (0 to 1 minute in the time axis of the EEG data — not shown here) affects the estimation of the *T*-index values for the subsequent 10 minutes (see stimulus artifact shaded area in this figure) Desynchronization of brain dynamics (*T*-index above T_{th} = 2.662) is observed thereafter, most significantly for 30 minutes after the stimulus.

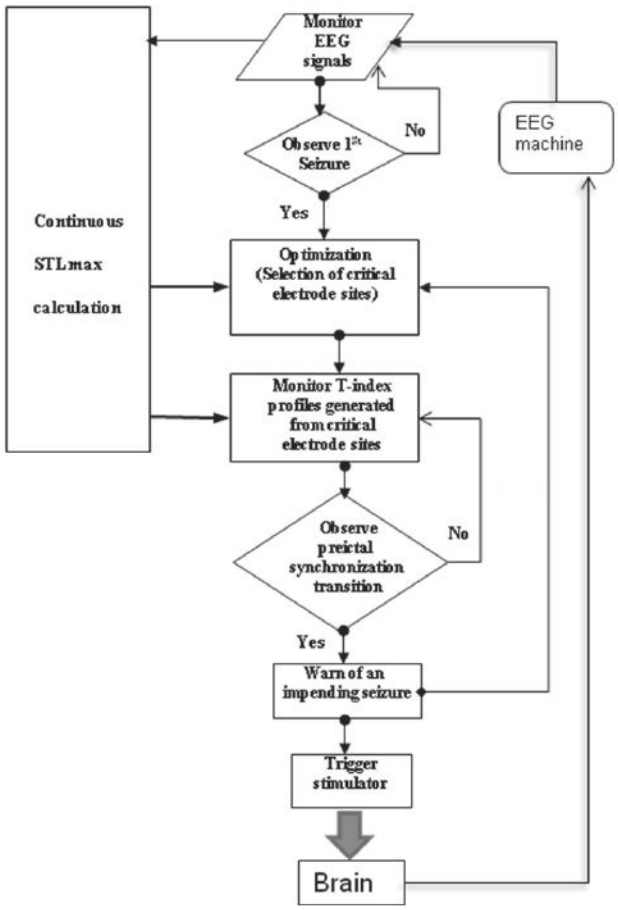

Fig. 3.

Flow chart of automated seizure prediction and control in the JIT stimulation system. Continuous realtime estimation of STL_{max} from EEG data is performed. Global optimization is employed to select the critical electrode sites at the first seizure and at seizure warnings thereafter. At seizure warning, the stimulator is triggered to deliver a predetermined stimulus.

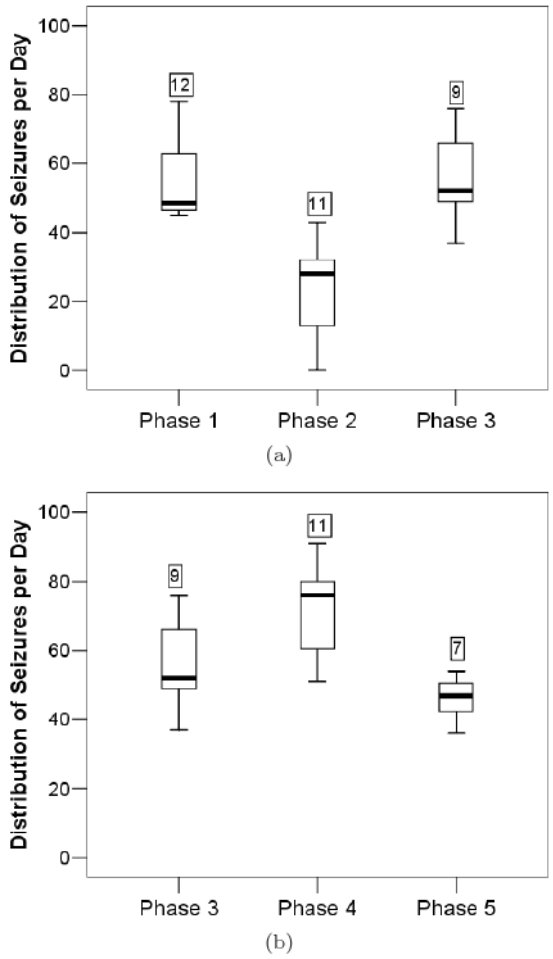

Fig. 4.

Just-in-time and periodic seizure control in Rat 2. The phases of the experiment are shown on the horizontal axis in order of occurrence. Upper panel: Baseline (Phase 1), JIT control (Phase 2), Baseline (Phase 3). The vertical axis represents the number of seizures occurring per day during each phase. In these Tukey's box-and-whisker plots, each box represents the interquartile range of the mean seizures per day, the black bar within the box represents the median of the seizure frequency, and the bottom and top whiskers represent 1.5 times below and above the lower and upper quartiles respectively. The number above each box represents the number of days the rat was in each phase of the experiment. A statistically significant decrease of seizure frequency is observed during JIT stimulation (Phase 2) in this rat. Lower panel: Baseline (Phase 3), P control (Phase 4), Baseline (Phase 5). Increase of seizure frequency is observed during periodic stimulation (Phase 4) in this rat.

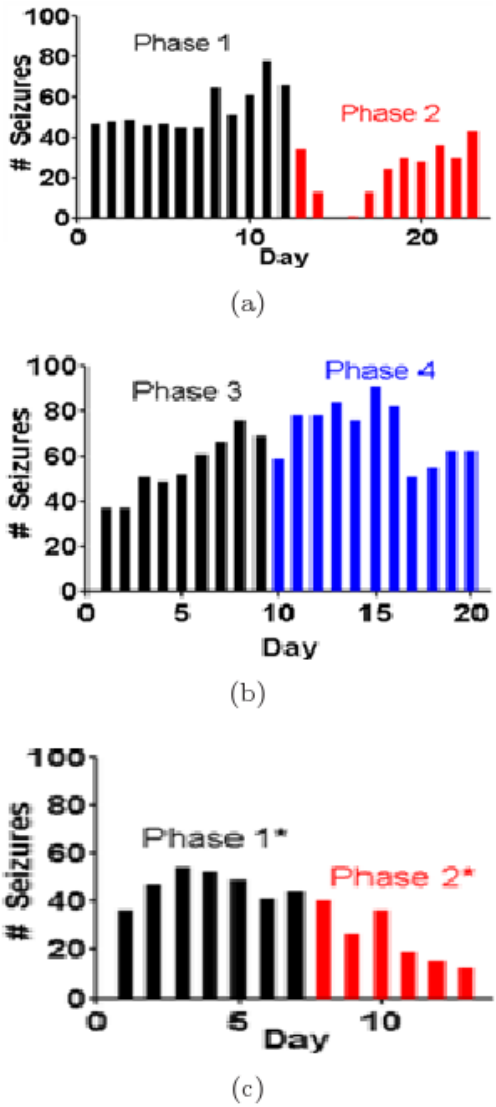

Fig. 5.

Seizure Frequency (number of seizures per day) in Rat 2 over: (a) Baseline and JIT periods (Phases 1 and 2 respectively), (b) Baseline and Periodic stimulation periods (Phases 3 and 4 respectively), and (c) Baseline and repetition of JIT periods (Phases 1* and 2* respectively; that is, phases 1 and 2 for Rat 2* in the Tables). Phase 2*, the repeat of JIT stimulation in Rat 2, is only of 6 days in duration because the rat pulled the headpiece off on the 7th day and had to be sacrificed.

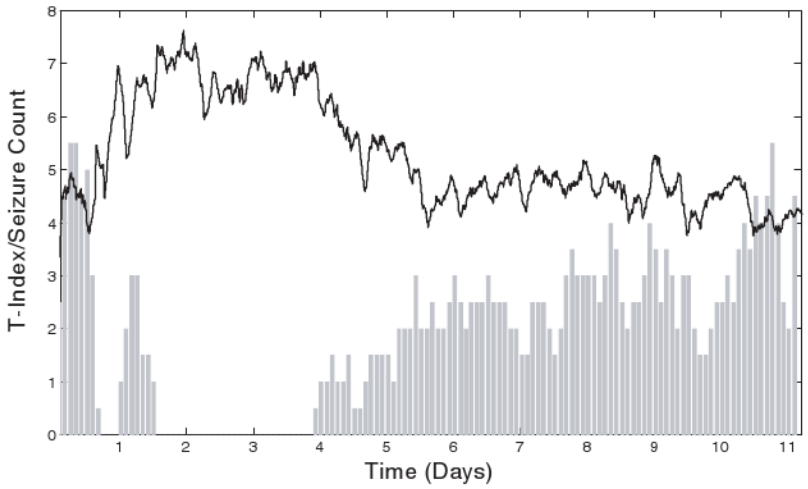

(a)

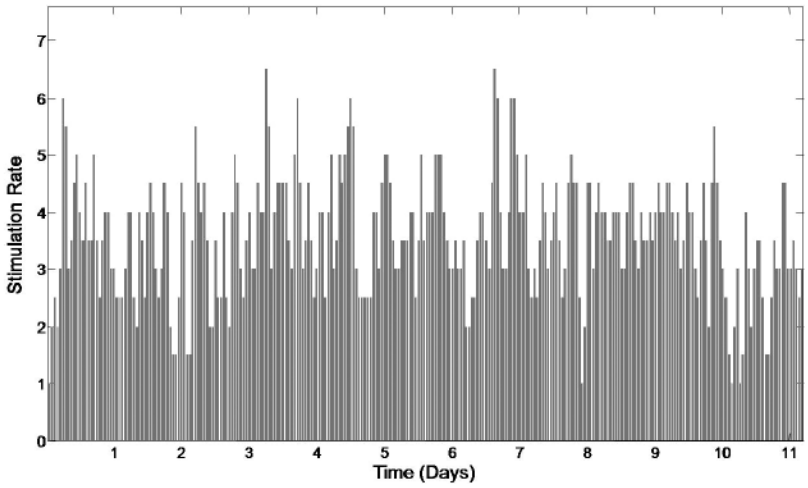

(b)

Fig. 6.

Brain dynamics of JIT seizure control in Rat 2 (Phase 2). (a) Top panel: The global *T*-index (solid black line) and the seizure frequency (# seizures in two-hour non-overlapping running windows — grey bars) are shown over time. It is observed that, when brain desynchronization (higher *T*-index values) exists, seizures are controlled (e.g. in days 1 to 4). However, when synchronization is higher (lower *T*-index values), seizure frequency is higher, which is indicative of ineffective seizure control. (b) Bottom panel: The delivered stimulus rate (#stimuli per 2 hour windows) over time.

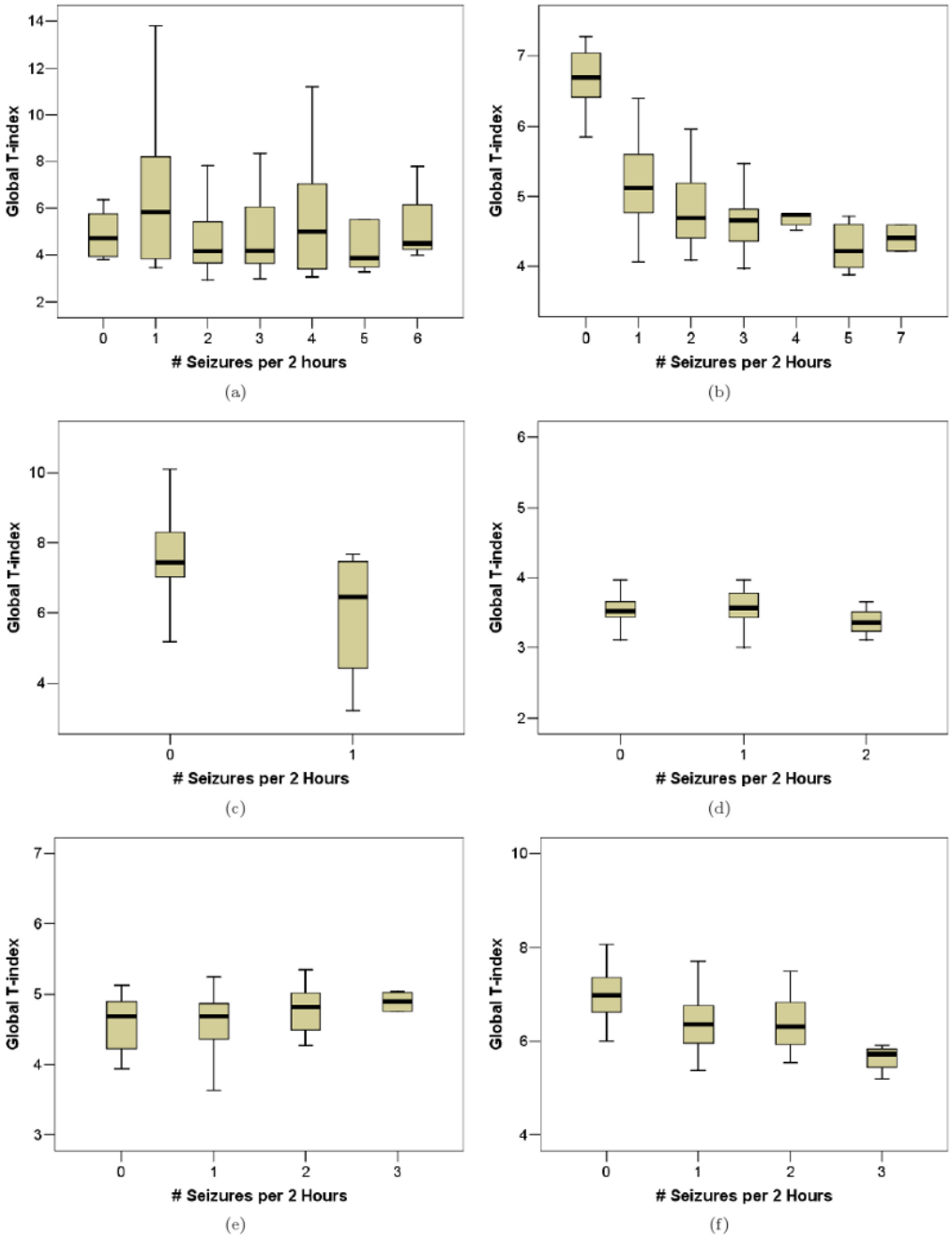

Fig. 7.

Global brain synchronization as a function of discrete seizure frequency (# seizures per 2-hour window) during JIT control stimulation for each rat. The global synchronization is estimated within the corresponding 2-hour windows and illustrated in box-and-whisker box format (see text for details). A significant increase in brain synchronization (lowering of mean global *T*-index with increasing seizure frequency) is apparent in Rats 2, 3, and 6 only (panels b, c, and f), while no significant change in brain synchronization with seizure frequency is observed in Rats 1, 4 and 5 (panels a, d, and e).

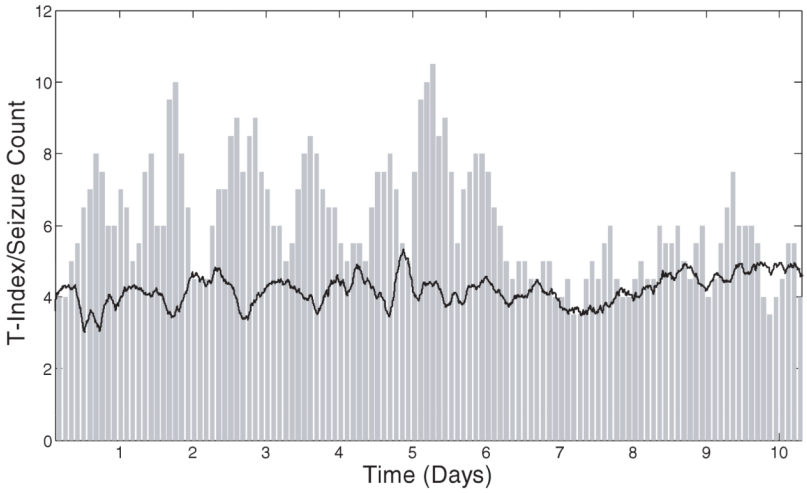

Fig. 8.

Brain dynamics of periodic seizure control in Rat 2 (Phase 4). The global *T*-index (solid black line) and the seizure frequency (# seizures in two-hour non-overlapping running windows — grey bars) are shown over time. Brain synchronization oscillates at high values and seizure frequency remains high throughout the record (no control of seizures is achieved).

Table 1

Duration (in Days) of each phase of the experiment.

Phase	1	2	3	4	5	Total (Days)
Rat 1	12	11	9	4	0	36
Rat 2	12	11	9	11	7	50
Rat 3	7	7	7	7	8	36
Rat 4	7	7	7	7	7	35
Rat 5	7	7	7	7	7	35
Rat 6	7	7	7	7	1	29
Total (Days)	52	50	46	43	30	221

Table 2

Stimulus amplitude and frequency for brain desynchronization in each rat.

	Amplitude (μA)	Frequency (Hz)
Rat 1	400	200
Rat 2	600	130
Rat 3	600	130
Rat 4	400	130
Rat 5	200	130
Rat 6	300	130

Table 3

Seizure data characteristics in training and testing datasets per rat (Phase 1).

	Rat 1		Rat 2		Rat 3		Rat 4		Rat 5		Rat 6	
	Train	**Test**	**Train**	**Test**	**Train**	**Test**	**Train**	**Test**	**Train**	**Test**	**Train**	**Test**
Recording length (hours)	153.3	153.3	129.6	129.6	83.3	83.3	83.3	83.3	83.3	83.3	84.7	84.7
# Seizures (747)	80	78	80	86	4	7	22	14	48	70	153	105
Mean interseizure interval (minutes)	111.6	117.0	156.3	91.8	1525.0	552.7	210.6	326.3	105.2	69.8	32.3	45.0

Table 4

Optimal prediction parameters from and performance of ESWP on the training datasets (Phase 1).

	Upper threshold (UT)	Tuple size (*k*)	Number of tuples (*l*)	# True predictions	Sensitivity	# False predictions	Specificity (/hr)	Mean prediction time (min)
Rat 1	3.5	2	5	73	0.924	16	0.104	66
Rat 2	4.0	2	5	55	0.696	23	0.177	67
Rat 3	4.5	2	3	2	0.667	3	0.036	67
Rat 4	3.5	2	4	15	0.714	4	0.048	43
Rat 5	3.5	2	3	40	0.851	12	0.144	65
Rat 6	3.5	2	5	66	0.434	1	0.012	24
Totals				251	0.659	59	0.096	55.3

Table 5

Performance of ESWP on testing datasets with optimal prediction parameters derived from the training datasets per rat (Phase 1).

	# SZs	# True predictions	Sensitivity	# False predictions	Specificity(per hr)	Mean prediction time (min)
Rat 1	77	71	0.922	36	0.235	61
Rat 2	85	69	0.812	10	0.077	64
Rat 3	6	5	0.833	3	0.036	54
Rat 4	13	11	0.846	28	0.336	89
Rat 5	69	58	0.841	19	0.228	70
Rat 6	104	50	0.481	5	0.059	44
Totals	354	264	0.746	101	0.164	63.7

Int J Neural Syst. Author manuscript; available in PMC 2011 June 22.

Table 6

JIT stimulation intervals.

	Mean stimulus interval(hours:min:sec)	Max stimulus interval(hours:min:sec)
Rat 1	0:17:35	4:50:19
Rat 2	0:16:45	1:55:32
Rat 3	0:29:19	2:01:41
Rat 4	0:22:42	1:45:59
Rat 5	0:32:02	2:07:50
Rat 6	0:35:53	3:38:36

Table 7

Performance of Just-in-time (JIT) stimulation for seizure control per rat (daily seizure frequency and seizure duration are given as mean ± standard deviation across days).

	# Seizures per day			Seizure duration (sec)		Average time of seizing per day in phase 1 (sec)	Average time of seizing per day in phase 2 (sec)
	Phase 1	JIT control phase 2	% Change	Phase 1	JIT control phase 2		
Rat 1	23.58 ± 2.52	29.09 ± 2.60	23.37	44.57 ± 1.26	44.63 ± 1.14	1051	1299
Rat 2	54.0 ± 3.12	22.91 ± 4.29	−57.57*	47.88 ± 0.80	53.83 ± 1.41^	2586	1233
Rat 2**	46.14 ± 2.39	24.67 ± 4.66	−46.53*	46.57 ± 1.95	40.93 ± 2.19	2149	1010
Rat 3	1.57 ± 0.78	0.57 ± 0.30	−63.69	89.8 ± 2.66	83.2 ± 1.93	141	47
Rat 4	5.29 ± 2.44	4.57 ± 0.81	−13.61	119.83 ± 8.90	79.56 ± 5.23^	634	364
Rat 5	17.14 ± 1.77	14.57 ± 1.86	−14.99	58.13 ± 1.45	50.24 ± 2.19^	996	732
Rat 6	37.14 ± 2.96	11.57 ± 1.70	−68.85*	73.17 ± 3.02	74.26 ± 4.64	2718	859

*Statistically significant with Wilcoxon sign-ranked test $p < 0.05$.

^Statistically significant with Kolmogorov-Smirnov Z test $p < 0.01$.

Table 8

Performance of Periodic (P) stimulation for seizure control per rat. (daily seizure frequency and seizure duration are given as mean ± standard deviation across days)

	# Seizures per day			Seizure duration (sec)		Average time of seizing per day in phase 3 (sec)	Average time of seizing per day in phase 4 (sec)
	Phase 3	JIT control phase 3	% Change	Phase 3	JIT control phase 4		
Rat 1	42.22 ± 4.14	21.75 ± 7.39	−48.48	38.86 ± 1.27	44.44 ± 2.46^	1641	967
Rat 2	55.33 ± 4.57	70.73 ± 4.02	27.83*	44.87 ± 0.91	38.72 ± 0.66^	2483	2739
Rat 3	1.57 ± 0.65	3.29 ± 0.97	109.55	100.45 ± 4.80	97.78 ± 3.95	158	322
Rat 4	5.57 ± 2.53	11.86 ± 1.64	112.93*	138.49 ± 9.51	73.07 ± 2.67^	771	867
Rat 5	26.57 ± 3.02	23.0 ± 2.37	−13.44	52.26 ± 1.63	48.51 ± 1.74	1389	1116
Rat 6	39.57 ± 7.29	20.14 ± 1.95	-49.10*	45.99 ± 2.24	59.94 ± 3.83^	1820	1207

*Statistically significant with Wilcoxon sign-ranked test $p < 0.05$.

^Statistically significant with Kolmogorov-Smirnov Z test $p < 0.01$.

+Rat 2** was not available for repetition of phase 3.